

The Kuramoto model on power law graphs

Georgi S. Medvedev* and Xuezhi Tang†

May 16, 2017

Abstract

The Kuramoto model (KM) of coupled phase oscillators on scale free graphs is analyzed in this work. The W -random graph model is used to define a convergent family of sparse graphs with power law degree distribution. For the KM on this family of graphs, we derive the mean field description of the system's dynamics in the limit as the size of the network tends to infinity. The mean field equation is used to study two problems: synchronization in the coupled system with randomly distributed intrinsic frequencies and existence and bifurcations of chimera states in the KM with repulsive coupling. The analysis of both problems highlights the role of the scale free network organization in shaping dynamics of the coupled system. The analytical results are complemented with the results of numerical simulations.

1 Introduction

Coupled dynamical systems on graphs serve as mathematical models of various technological physical, biological, social, and economic networks [33]. Examples include neuronal and genetic networks and models of flocking in life sciences [27]; power and information networks and consensus protocols in technology [26]; and economic and social networks and models of opinion dynamics in social sciences [33]. This list can be continued. Numerical simulations and mathematical analysis of coupled systems provided many important insights into the mechanisms underlying collective dynamics in complex networks. In the last two decades, there have been a remarkable progress in understanding classical phenomena such as synchronization and phase locking in complex networks [8, 35, 36, 24, 25], and the discoveries of new effects in the dynamics of networks such as chimera states [17, 1, 30]. The research on dynamical networks has been fueled by the desire for better understanding the link between the structure of a network and its dynamics. This is the main motivation of our work.

Real world networks feature a rich variety of connectivity patterns. Scale free networks have been singled out in the network science community for their nontrivial structure and compelling applications. The latter include the world wide web and scientific citation network among other physical, biological, and social networks [2]. Scale free graphs are characterized by power law asymptotics of the degree distribution.

*Department of Mathematics, Drexel University, 3141 Chestnut Street, Philadelphia, PA 19104; medvedev@drexel.edu

†Wells Fargo Securities, 505 S. Tryon street, Charlotte, NC 28202; xuezhi.tang@wellsfargo.com

For this reason, they are also called power law graphs. In practice, power law distribution is determined by statistical methods. Different combinatorial algorithms such as the preferential attachment (see, e.g., [5]) and Chung-Lu [9] methods are used to generate computational models of scale free graphs. Dynamical systems on the graphs generated by these methods are difficult to study analytically. Consequently, there are few mathematical results on the dynamics of coupled systems on scale free graphs. The goal of this paper is to rectify this situation. We introduce a framework for modeling and analyzing coupled systems on scale free graphs. Further, we illustrate the role that the scale free connectivity can play in shaping dynamics of coupled systems. To this end, we analyze two problems: synchronization in attractively coupled KM on power law graphs with randomly distributed intrinsic frequencies and chimera states in repulsively coupled KM.

The KM of coupled phase oscillators is one of the most successful mathematical models for studying collective dynamics and synchronization [18]. It captures the essential features of dynamics of weakly coupled limit cycle oscillators [13] and has many interesting applications in physical and biological sciences [35]. In the synchronization problem, the intrinsic frequencies of the individual oscillators are assumed to be taken from a probability distribution with density function g . Then one wants to find a critical value of the coupling strength, which marks the transition from stochastic distribution of the phases of oscillators to synchronization. For the classical KM on complete graphs, Kuramoto found the critical value $K_c = 2\pi/g(0)$. Kuramoto's self-consistent analysis recently received a rigorous mathematical justification in [8, 6]. In the present paper, we use the results in [7], which extend some of the techniques from [8] to the KM on graphs. Using these techniques, we obtain an explicit formula for the onset of synchronization for scale free graphs.

The second problem considered in this paper deals with chimera states. These are special spatio-temporal patterns in dynamical networks, which feature coexisting regions of synchronous (regular) and stochastic behaviors. Chimera states were discovered by Kuramoto and Battogtokh in the KM with random initial conditions [17, 1]. Since then they have been studied in different settings. Importantly, chimera states have been confirmed experimentally (see, e.g., [29]). In the last decade, chimera states have become a subject of intense research [32]. In this paper, we present a new simple mechanism for chimera states in the KM with repulsive coupling. Our mechanism exploits the scale free structure of the network and admits a simple and explicit analytical description.

The organization of the paper is as follows. In the next section, we explain the W-random graph model of power law graphs, which will be used in this work. There we will also formulate the KM on the power law graphs following [15]. In Section 3, we review the mathematical background of the mean field equation for the KM on graphs following [7]. Although, the results in [7] do not apply to the model on the power law graphs due to the singularity in this graph model, they can be used for the truncated power law model. The latter captures all essential features of the original model Section 4 deals with the synchronization problem for the KM on power law graphs, and Section 5 – with the chimera states in the repulsively coupled model. We conclude with brief discussion in Section 6.

2 The model

W-random graphs provide a convenient framework for deriving the continuum limit of the KM on convergent families of graphs [22, 23, 15, 7]. In this section, we explain the W-random graph model adapted from [4]

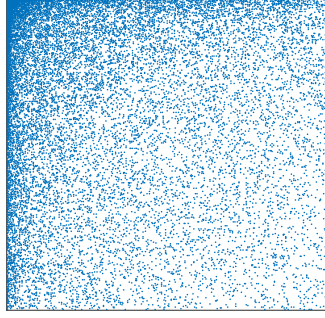


Figure 1: The pixel plot of the adjacency matrix of a power law graph.

that will be used below.

Let $W(x, y) = (xy)^{-\alpha}$ for some $\alpha \in (0, 1)$,

$$X_n = \{x_{n0}, x_{n1}, x_{n2}, \dots, x_{nn}\}, \quad x_{ni} = i/n, \quad i = 0, 1, \dots, n, \quad (2.1)$$

and $\rho_n = n^{-\beta}$, $\alpha < \beta < 1$.

$\Gamma_n = G(W, \rho_n, X_n)$ stands for a random graph with the node set $V(\Gamma_n) = [n]$ and the edge set $E(\Gamma_n)$ defined as follows. The probability that $\{i, j\}$ forms an edge is

$$\mathbb{P}(\{i, j\} \in E(\Gamma_n)) = \rho_n \bar{W}_n(x_{ni}, x_{nj}), \quad i, j \in [n], \quad (2.2)$$

where

$$\bar{W}_n(x, y) = \rho_n^{-1} \wedge W(x, y).^1 \quad (2.3)$$

The decision whether a given pair of nodes is included in the edge set is made independently from other pairs. In other words, $G(W, \rho_n, X_n)$ is a product probability space

$$(\Omega_n = \{0, 1\}^{n(n+1)/2}, 2^{\Omega_n}, \mathbb{P}). \quad (2.4)$$

By $\Gamma_n(\omega), \omega \in \Omega_n$, we will denote a random graph drawn from the probability distribution $G(W, \rho_n, X_n)$.

Lemma 2.1. [15] $\Gamma_n = G(W, \rho_n, X_n)$ has the following properties:

A) The expected degree of node $i \in [n]$ of Γ_n is²

$$\mathbb{E}_\omega \deg_{\Gamma_n}(i) = (1 - \alpha)^{-1} n^{1+\alpha-\beta} i^{-\alpha} (1 + o(1)). \quad (2.5)$$

B) The expected edge density of Γ_n is $(1 - \alpha)^{-2} n^{-\beta} (1 + o(1))$.

¹Throughout this paper, we use $a \wedge b$ and $a \vee b$ to denote $\min\{a, b\}$ and $\max\{a, b\}$ respectively.

²Here and below, \mathbb{E}_ω denotes the mathematical expectation with respect to the probability space (2.4) underlying the random graph model.

Let $\Gamma_n = \Gamma_n(\omega)$, $\omega \in \Omega_n$, be a random graph model taken from the probability distribution $G(W, \rho_n, X_n)$. The KM on Γ_n is defined as follows:

$$\dot{u}_{ni} = \phi_i + \frac{K}{n\rho_n} \sum_{j=1}^n \xi_{nij}(\omega) \sin(u_{nj} - u_{ni}), \quad i \in [n], \quad (2.6)$$

where ϕ_i is the intrinsic frequency of the oscillator i , $\xi_{nij}(\omega) = \mathbf{1}_{E(\Gamma_n(\omega))}(\{i, j\})$ is a Bernoulli random variable, which takes value 1 when $\{i, j\}$ is an edge of Γ_n . K controls the strength of coupling. The scaling factor ρ_n on the right hand side of (2.6) is used to guarantee that the (2.6) has a nontrivial continuum limit as $n \rightarrow \infty$. In the classical KM on complete graph $\rho_n = 1$. The same holds for the KM on any dense graphs (i.e., the graph for which the edge density remains $O(1)$ for $n \gg 1$). However, for sparse graphs like the power law graph $\Gamma_n = G(W, \rho_n, X_n)$, the edge density vanishes as $n \rightarrow \infty$ (cf. Lemma 2.1). Thus, the scaling of the right hand side of (2.6) by ρ_n is needed, if one wants to have a nondegenerate continuum limit as $n \rightarrow \infty$.

The KM (2.6) is derived from a system of weakly coupled oscillators [18, 13]. The dynamical variable u_{ni} stands for the phase of oscillator i and ϕ_i is its intrinsic frequency. Until Section 5, we assume that the intrinsic frequencies are drawn from a continuous probability distribution with density g . The right hand side of (2.6) depends on the realization of the random graph model $\Gamma_n = G(W, \rho_n, X_n)$. Thus, we are dealing with a system of ordinary differential equations with random coefficients. As a first step in analyzing (2.6), we substitute (2.6) by the averaged model, which approximates the random KM (2.6). Specifically, we average the right-hand side of (2.6) over all possible realizations of Γ_n :

$$\dot{v}_{ni}(t) = F_{ni}(v_n), \quad v_n(t) = (v_{n1}(t), v_{n2}(t), \dots, v_{nn}(t)), \quad (2.7)$$

where

$$\begin{aligned} F_{ni}(v) &= \mathbb{E}_\omega \left\{ \phi_i + K(n\rho_n)^{-1} \sum_{j=1}^n \xi_{nij}(\omega) \sin(u_{nj} - u_{ni}) \right\} \\ &= \phi_i + K(n\rho_n)^{-1} \sum_{j=1}^n \mathbb{E}_\omega (\xi_{nij}(\omega)) \sin(u_{nj} - u_{ni}) \\ &= \phi_i + Kn^{-1} \sum_{j=1}^n \bar{W}_{nij} \sin(u_{nj} - u_{ni}), \end{aligned}$$

where we used (2.2). Recall that \mathbb{E}_ω stands for the mathematical expectation with respect to the probability space (2.4).

Thus, the averaged KM has the following form

$$\dot{v}_{ni} = \phi_i + Kn^{-1} \sum_{j=1}^n \bar{W}_{nij} \sin(v_{nj} - v_{ni}). \quad (2.8)$$

It is shown in [7] (see also [15]) that for $n \gg 1$, solutions of the initial value problems (IVPs) for the original and averaged KMs subject to the same initial conditions remain close on finite time intervals with probability 1.

Lemma 2.2. [7]

$$\lim_{n \rightarrow \infty} \max_{t \in [0, T]} \|v_n(t) - u_n(t)\|_{2,n} = 0 \quad \text{almost surely.} \quad (2.9)$$

Here,

$$\|v_n\|_{2,n} := \sqrt{n^{-1} \sum_{i=1}^n v_{ni}^2} \quad (2.10)$$

is the discrete L^2 -norm.

3 The mean field limit

Our main tool for studying the KM in this paper is the mean field equation. It is derived in the limit as the number of oscillators tends to infinity. In this section, we explain the mathematical basis of the mean field limit for the model at hand.

In studies of large groups of interacting dynamical systems, it is often useful to take the limit as the size of system goes to infinity [11]. The continuum limit has been instrumental in the analysis of synchronization and chimera states in the KM [35, 30]. For the discrete model (2.8), the continuum limit has the following form

$$\frac{\partial}{\partial t} \rho(t, u, \phi, x) + \frac{\partial}{\partial u} \{ \rho(t, u, \phi, x) V(t, u, \phi, x) \} = 0 \quad (3.1)$$

where

$$V(t, u, \phi, x) = \phi + K \int_I \int_{\mathbb{R}} \int_{\mathbb{S}} W(x, y) \sin(v - u) \rho(t, v, \phi, y) dv d\phi dy \quad (3.2)$$

Here, $\rho(t, u, \phi, x)$ stands for a probability density function on $G = \mathbb{S} \times \mathbb{R} \times I$ parametrized by time $t \in \mathbb{R}^+$. It aims to describe the distribution of the oscillators of the discrete model (2.6) at time t , provided both IVPs for (2.6) and (3.1) are initialized appropriately.

For the original KM on complete graphs, the rigorous mathematical justification of the mean field equation (3.1) was given by Lancellotti [19]. It relies on the classical theory for the Vlasov equation [28]. For the KM on graphs, the justification of the mean field limit was developed in [7]. The analysis in [7] uses Lipschitz continuity of W and does not apply to the singular kernel $W(x, y) = (xy)^{-\alpha}$ used in this paper. However, if W is replaced by the truncated kernel $W_C(x, y) = C \wedge (xy)^{-\alpha}$ for arbitrary $C > 0$ then the interpretation of the mean field limit in [7] carries over to the problem at hand. Using the truncated kernel does not limit the applications of our results, as all effects considered in this work can be achieved with W_C instead of W . Thus, in the remainder of this section, we explain the mathematical meaning of the mean field equation (3.1) and its relation to the discrete system (2.8) assuming that $W := W_C$ for sufficiently large $C > 0$.

Consider the following initial condition for (3.1)

$$\rho(0, u, \phi, x) = \rho^0(u, \phi, x)g(\phi), \quad (3.3)$$

where the nonnegative $\rho^0 \in L^1(G)$ satisfies

$$\int_{\mathbb{S}} \rho^0(u, \phi, x) du = 1 \quad \forall (\phi, x) \in \mathbb{R} \times I. \quad (3.4)$$

Then, as shown in [7], there is a unique weak solution of the IVP (3.1), (3.3). Moreover, $\rho(t, \cdot)$ is a probability density function on G for every $t \in [0, T]$. Thus, one can define the probability measure

$$\mu_t(A) = \int_A \rho(t, u, \phi, x) du d\phi dx, \quad A \in \mathcal{B}(G), \quad (3.5)$$

where $\mathcal{B}(G)$ stands for the collection of Borel subsets of G .

On the other hand, the solution of the IVP for discrete problem (2.8) defines the empirical measure

$$\mu_t^n(A) = n^{-1} \sum_{i=1}^n \mathbf{1}_A(\theta_{ni}(t), \phi_i, x_{ni}), \quad A \in \mathcal{B}(G). \quad (3.6)$$

The analysis in [7], based on the Neunzert's theory for Vlasov equation (cf. [28]), shows that

$$\sup_{t \in [0, T]} d(\mu_t^n, \mu_t) \rightarrow 0 \quad \text{as } n \rightarrow \infty, \quad (3.7)$$

provided

$$d(\mu_0^n, \mu_0) \rightarrow 0 \quad \text{as } n \rightarrow \infty, \quad (3.8)$$

Here, $d(\cdot, \cdot)$ stands for the bounded Lipschitz distance, which metrizes weak convergence for the space of Borel probability measures on G [10]. Thus, if the initial distribution of oscillators (i.e., the initial conditions for (2.8)) converges weakly to μ_0 as $n \rightarrow \infty$, then the solution of the continuous problem (3.1), (3.3) approximates the distribution of oscillators around \mathbb{S} for every $t \in [0, T]$. The same applies to the empirical measures generated by the discrete model on random graph (2.6) via Lemma 2.2 (cf. [7]).

4 Synchronization

With the mean field limit (3.1) in hand, we are equipped to study dynamics of the KM on power law graphs (2.6). First, note that $\rho(t, u, \phi, x) = (2\pi)^{-1}g(\omega)$ is a probability density on G , corresponding to the state of the network with all oscillators distributed uniformly around \mathbb{S} , which will be referred to as the incoherent state. It is a solution of (3.1).

To study stability of the incoherent state, we use the results of [7]. To this end, throughout this section, we assume that $\alpha \in (0, 1/2)$ and the probability density function g characterizing the distribution of intrinsic frequency ϕ is even.

Next, consider a self-adjoint operator $\mathcal{W} : L^2(I) \rightarrow L^2(I)$ defined by

$$\mathcal{W}[f] = \int_I W(\cdot, y) f(y) dy, \quad f \in L^2(I). \quad (4.1)$$

We will need the spectral properties of \mathcal{W} summarized in the following lemma.

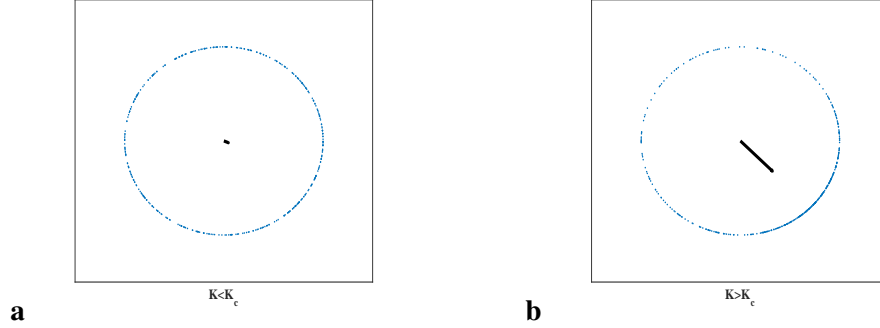


Figure 2: The distribution of the oscillators for the values of the coupling strength below (a) and above (b) the synchronization threshold. The black arrows indicate the order parameter in each case.

Lemma 4.1. For $\alpha \in (0, 1/2)$, the spectrum of \mathcal{W} consists of a simple eigenvalue $(1 - 2\alpha)^{-1}$ and the zero eigenvalue of infinite multiplicity.

Proof. Suppose ζ is an EV of \mathcal{W} , and $f \in L^2(I)$ is a corresponding eigenfunction. Then

$$x^{-\alpha} \int_I y^{-\alpha} f(y) dy = \zeta f(x).$$

If f is orthogonal to the subspace of $L^2(I)$ spanned by $x^{-\alpha}$, then $\zeta = 0$. Otherwise, f must be equal to $Cx^{-\alpha}$ for some $C \neq 0$ and

$$\zeta = \int_I y^{-2\alpha} dy = (1 - 2\alpha)^{-1}.$$

□

By [7, Theorem 3.4], the incoherent state $\rho = (2\pi)^{-1}g(\omega)$ is linearly stable for $K \leq K_c$, where the critical coupling strength

$$K_c = \frac{2}{\pi g(0) \zeta_{max}(\mathcal{W})}, \quad (4.2)$$

and $\zeta_{max}(\mathcal{W})$ is the largest positive eigenvalue of \mathcal{W} . Using (4.2) and Lemma 4.1, we conclude that the onset of synchronization for the KM on scale free graphs is defined by the critical value

$$K_c = \frac{2(1 - 2\alpha)}{\pi g(0)}, \quad \alpha \in (0, 1/2). \quad (4.3)$$

In particular, for the Gaussian density $g(\phi) = e^{-\phi^2/2}/\sqrt{2\pi}$, we have

$$K_c(\alpha) = 2\sqrt{\frac{2}{\pi}}(1 - 2\alpha).$$

For $K \leq K_c$, the incoherent state is linearly stable and the oscillators are distributed approximately uniformly around \mathbb{S} (see Fig. 2a). For values of $K > K_c$, numerics shows a gradual buildup of coherence in the system dynamics (see Fig. 2b). Note that the synchronization threshold (4.3) can be made arbitrarily small by taking α close $1/2$. Such good synchronizability of the network is an implication of the scale free connectivity.

5 Repulsive coupling

In the previous section, we found that the incoherent state is stable for $K \leq K_c$ and is unstable otherwise. For $K > K_c$, coherence gradually builds up and the asymptotic state of the system becomes closer and closer to complete synchronization as $K \rightarrow \infty$. In this section, we focus on pattern formation in repulsively coupled networks, i.e., we consider (2.6) for $K < 0$. In this case, the incoherent state is stable, but as we will see below, there are other stable states. To make the model analytically tractable, we set the intrinsic frequencies equal to the same value $\phi_i = \phi$, $i \in [n]$. By switching to a uniformly rotating frame of coordinates, without loss of generality we assume $\phi = 0$.

Thus, in the remainder of this section, we will be dealing with the following model

$$\dot{u}_{ni} = (n\rho_n)^{-1} \sum_{j=1}^n \xi_{nij}(\omega) \sin(u_{ni} - u_{nj}), \quad i \in [n]. \quad (5.1)$$

Here, we set K to -1 , since this can always be achieved by rescaling time.

The averaged model then becomes

$$\dot{v}_{ni} = n^{-1} \sum_{j=1}^n \bar{W}_{nij} \sin(v_{ni} - v_{nj}), \quad i \in [n]. \quad (5.2)$$

The corresponding mean field equation is given by

$$\frac{\partial}{\partial t} \rho(t, u, x) + \frac{\partial}{\partial u} \{V(t, u, x) \rho(t, u, x)\} = 0, \quad (5.3)$$

where

$$V(t, u, x) = \int_{\mathbb{S}} \int_I W(x, y) \sin(u - v) \rho(t, v, y) dv dy. \quad (5.4)$$

The synchronous state is always unstable for the KM with repulsive coupling on any undirected graph (cf. [24, Theorem 3.7]). Thus, it is unstable for the KM on power law graphs (5.1). The proof of this fact uses a variational argument. A similar variational principle applies to the averaged model (5.2). It is used in the next subsection to identify attractors in the repulsively coupled model.

5.1 The Lyapunov function

For the classical KM on complete graphs, Kuramoto introduced the order parameter

$$R_{cmp}(u) = n^{-1} \sum_{j=1}^n e^{iu_j}, \quad u = (u_1, u_2, \dots, u_n) \in \mathbb{S}^n. \quad (5.5)$$

to study the transition to synchronization [18]. The complex-valued order parameter (5.5) provides a convenient measure of coherence in the system dynamics. Indeed, if the phases u_i , $i \in [n]$, are distributed around \mathbb{S} uniformly then $|R_{cmp}(u)| \approx 0$, whereas if they evolve in synchrony then $|R_{cmp}(u)| \approx 1$.

For the KM on weighted graphs (5.2), there is a suitable generalization of the order parameter:

$$R(u) = n^{-1} \sum_{j=1}^n a_{nj} e^{iu_j}, \quad a_{ni} = x_{ni}^{-\alpha}, \quad i \in [n]. \quad (5.6)$$

Using R , (5.2) can be rewritten as follows

$$\dot{u}_{ni} = a_{ni} |R(u_n)| \sin(u_{ni} - \psi), \quad i \in [n], \quad (5.7)$$

where $\psi = \text{Arg } R(u_n)$. As follows from (5.7), there are two classes of equilibria of (2.8):

$$\begin{aligned} \mathcal{E}_{n,1} &= \{u \in \mathbb{S}^n : (R(u) \neq 0) \ \& \ (u_j - u_i \in \{0, \pi\}, \ i, j \in [n])\}, \\ \mathcal{E}_{n,2} &= \{u \in \mathbb{S}^n : R(u) = 0\}. \end{aligned}$$

Theorem 5.1. *The ω -limit set of (2.8) is $\mathcal{E}_{n,1} \cup \mathcal{E}_{n,2}$.*

Proof. Let

$$L(u) = \frac{1}{2n} |R(u)|^2 \quad (5.8)$$

and note that

$$\begin{aligned} 2nL(u) &= \left[n^{-1} \sum_{j=1}^n a_{nj} \cos u_{nj} \right]^2 + \left[n^{-1} \sum_{j=1}^n a_{nj} \sin u_{nj} \right]^2 \\ &= n^{-2} \sum_{i,j=1}^n a_{ni} a_{nj} \cos(u_{ni} - u_{nj}) \end{aligned} \quad (5.9)$$

Further,

$$\frac{\partial}{\partial u_i} L(u) = -n^{-1} \sum_{j=1}^n \sin(u_{ni} - u_{nj}). \quad (5.10)$$

Thus, (5.7) is a gradient system

$$\dot{u}_n = -\nabla L(u_n).$$

and

$$\dot{L} = (\nabla L(u_n), \dot{u}_n) = - \sum_{i=1}^n \left(n^{-1} \sum_{j=1}^n a_{ni} |R(u_n)| \sin(u_{ni} - \psi) \right)^2 \leq 0. \quad (5.11)$$

By the Barbashin-Krasovskii-Lassale extension of the Lyapunov's direct method [3, 16, 20], we conclude that the ω -limit set of (2.8) is the set of equilibria $\mathcal{E}_{n,1} \cup \mathcal{E}_{n,2}$. \square

5.2 Stability of equilibria in $\mathcal{E}_{n,1}$

In this subsection, to gain first insights into the asymptotic states of the repulsively coupled KM, we study stability of phase locked steady states of (5.7).

By the definition of $\mathcal{E}_{n,1}$, for $u = (u_1, u_2, \dots, u_n) \in \mathcal{E}_{n,1}$ we have $u_j - u_i \in \{0, \pi\}$, $i, j \in [n]$. Thus, up to translation by a constant vector

$$\mathcal{E}_{n,1} = \bigcup_{m=1}^n \mathcal{E}_{n,1}^{(m)},$$

where $\mathcal{E}_{n,1}^{(m)}$ consists of equilibria with precisely m coordinates equal to 0 and the rest to π . For example,

$$\underbrace{(0, 0, \dots, 0)}_m, \underbrace{(\pi, \pi, \dots, \pi)}_{n-m} \in \mathcal{E}_{n,1}^{(m)}. \quad (5.12)$$

Suppose $u_n^{(m)} = (u_{n,1}^{(m)}, u_{n,2}^{(m)}, \dots, u_{n,n}^{(m)}) \in \mathcal{E}_{n,1}^{(m)}$ for some $m \in [n]$. Then there is an m -element subset $\Lambda_n^{(m)} \subset [n]$, $|\Lambda_n^{(m)}| = m$ such that

$$u_{n,i}^{(m)} = \begin{cases} 0, & i \in \Lambda_n^{(m)}, \\ \pi, & i \notin \Lambda_n^{(m)}. \end{cases} \quad (5.13)$$

Denote the matrix of linearization of (5.1) about $u_n^{(m)}$ by A . A straightforward computation shows that

$$A = D - vv^T, \quad (5.14)$$

where $D = (d_{ij})$ is a diagonal matrix with nonzero entries

$$d_{ii} = \begin{cases} x_{ni}^{-\alpha} d, & i \in \Lambda_n^{(m)}, \\ -x_{ni}^{-\alpha} d, & i \notin \Lambda_n^{(m)}, \end{cases} \quad d := n^{-1} \sum_{j=1}^n (-1)^{\sigma(j)} x_{nj}^{-\alpha}, \quad (5.15)$$

$$v = \left((-1)^{\sigma(1)} x_{n1}^{-\alpha}, (-1)^{\sigma(2)} x_{n2}^{-\alpha}, \dots, (-1)^{\sigma(n)} x_{nn}^{-\alpha} \right), \quad \sigma(i) = \begin{cases} 0, & i \in \Lambda_n^{(m)}, \\ 1, & i \notin \Lambda_n^{(m)}. \end{cases} \quad (5.16)$$

Lemma 5.2. *Let $u \in \mathcal{E}_{n,1}^{(m)}$, $m \in [n]$.*

If $d > 0$ then the matrix of linearization about $u_n^{(m)}$, A , has at least $m - 1$ positive eigenvalues of D , at least $n - m - 1$ negative eigenvalues, and at least one zero eigenvalue.

If $d < 0$, A has at least $n - m - 1$ positive eigenvalues of D , at least $m - 1$ negative eigenvalues, and at least one zero eigenvalue.

Corollary 5.3. *All equilibria from $\mathcal{E}_{n,1}^{(m)}$, $1 < m \leq n$, are unstable. In particular, all solutions of the form (5.12) are unstable for $m > 1$.*

Proof of Lemma 5.2. Suppose $d > 0$. Let $\lambda_k(D)$ and $\lambda_k(A)$ denote the eigenvalues of D and A arranged in the increasing order counting multiplicity. By the interlacing inequalities (cf. [14, Theorem 4.3.4]), we have

$$\lambda_{n-m-1}(A) \leq \lambda_{n-m}(D) < 0,$$

and

$$0 < \lambda_{n-m+1}(D) \leq \lambda_{n-m+2}(A).$$

Finally, there is at least one zero eigenvalue of A , because its rows sum to 0.

The case $d < 0$ is analyzed similarly. □

5.3 The Ott-Antonsen Ansatz

Unlike equilibria in $\mathcal{E}_{n,1}$ considered in the previous subsection, equilibria in $\mathcal{E}_{n,2}$ are harder to identify explicitly. To study properties of the equilibria in $\mathcal{E}_{n,2}$, we will invoke the mean field equation:

$$\frac{\partial}{\partial t} \rho(t, u, x) + \frac{\partial}{\partial u} \{V(t, u, x) \rho(t, u, x)\} = 0, \quad (5.17)$$

where

$$V(t, u, x) = \int_I \int_{\mathbb{S}} W(x, y) \sin(u - v) \rho(t, v, y) dv dy. \quad (5.18)$$

To identify a class of stable steady states of (5.17), we employ the Ott-Antonsen Ansatz [31], i.e., we look for solutions of (5.17) in the following form:

$$\rho(t, u, x) = \frac{1}{2\pi} \left(1 + \sum_{k=1}^{\infty} \left(\overline{z(t, u)}^k e^{iku} + z(t, u)^k e^{-iku} \right) \right). \quad (5.19)$$

If $\sup_{x \in I, t \in [0, T]} |z(t, x)| < 1$ the series on the right hand side of (5.19) is absolutely convergent. Plugging (5.19) into (5.17), after straightforward albeit tedious manipulations, one verifies that (5.19) solves (5.17), provided $z(t, x)$ satisfies the following equation

$$\frac{\partial}{\partial t} z(t, x) = \frac{1}{2x^\alpha} (z(t, x)^2 - 1) \mathcal{R}[z(t, \cdot)], \quad (5.20)$$

where

$$\mathcal{R}[v] = \int_I y^{-\alpha} v(y) dy. \quad (5.21)$$

From (5.19), it follows that

$$z(t, x) = \int_0^{2\pi} \rho(t, u, x) e^{iu} du. \quad (5.22)$$

Using (5.22), we can express $\mathcal{R}[z]$ in terms of the density ρ :

$$\mathcal{R}[z] = \int_I \int_{\mathbb{S}} y^{-\alpha} \rho(t, u, y) e^{iu} du dy, \quad (5.23)$$

i.e., \mathcal{R} is the continuous counterpart of the order parameter (5.6).

In the remainder of this section, we restrict to real solutions of (5.20). It is instructive to review the interpretation of $z(t, x)$ (cf. [30]). To this end, note that (5.19) implies

$$\rho(t, u, x) = \frac{1 - |z(t, x)|^2}{2\pi (1 - 2|z(t, x)| \cos(u - \text{Arg } z(t, x)) + |z(t, x)|^2)}. \quad (5.24)$$

In particular, $z \equiv 0$ corresponds to the uniform density, while values of z close to ± 1 indicate that the density is concentrated around 0 and π respectively.

5.4 The nonlocal equation

Let $\mathcal{M}(0, 1)$ be a space of measurable functions $z : (0, 1] \rightarrow [-1, 1]$. In analogy to the discrete model (5.1), we divide the equilibria of (5.20) into two classes:

$$\tilde{\mathcal{E}}_1 = \{z \in \mathcal{M}(0, 1) : (|z(x)| = 1, x \in (0, 1]) \& (\mathcal{R}[z] \neq 0)\}, \quad \tilde{\mathcal{E}}_2 = \{z \in \mathcal{M}(0, 1) : \mathcal{R}[z] = 0\}.$$

Theorem 5.4. *Let $z_0 \in \mathcal{M}(0, 1)$ and $z_0 \notin \tilde{\mathcal{E}}_1$. Then the ω -limit set of the trajectory of (5.20) starting at z_0 , $\omega(z_0) \in \tilde{\mathcal{E}}_2$.*

Proof. Suppose $\mathcal{R}(0) := \mathcal{R}[z(0, \cdot)] > 0$. Changing the time variable to $t = \phi(\tau)$ subject to

$$\phi'(\tau) = \frac{1}{\int_I y^{-\alpha} \tilde{z}(\tau, y) dy}, \quad \tilde{z}(\tau, y) := z(\phi(\tau), x), \quad \phi(0) = 0, \quad (5.25)$$

we reduce (5.20) to

$$\frac{\partial}{\partial \tau} \tilde{z} = \frac{1}{2x^\alpha} (\tilde{z}^2 - 1). \quad (5.26)$$

The last equation is integrated explicitly

$$\tilde{z}(\tau, x) = \frac{1 - C(x) \exp\{\frac{\tau}{x^\alpha}\}}{1 + C(x) \exp\{\frac{\tau}{x^\alpha}\}}, \quad C(x) = \frac{1 - z_0(x)}{1 + z_0(x)}. \quad (5.27)$$

Clearly, $\tilde{z}(\tau, x) \searrow -1$ for $x \in I$ as $\tau \rightarrow \infty$. Thus, there is $0 < \tau^* < \infty$ such that $\tilde{\mathcal{R}}(\tau^*) := \tilde{\mathcal{R}}[\tilde{z}(\tau^*, \cdot)] = 0$ and $\tilde{\mathcal{R}}(\tau) > 0$ for $\tau \in [0, \tau^*)$.

The change of time (5.25) is well defined for $\tau \in [0, \tau^*)$. In terms of the original time, we have the description of the system's dynamics on the time interval $[0, t^*)$, with

$$t^* = \lim_{\tau \rightarrow \tau^* - 0} \int_0^\tau (\tilde{\mathcal{R}}(s))^{-1} ds. \quad (5.28)$$

Denote $\mathcal{R}(t) = \mathcal{R}[z(t, \cdot)]$. If $t^* < \infty$ then $\mathcal{R}(t) = \tilde{\mathcal{R}}(\tau^*) = 0$ for $t \geq t^*$. Otherwise, multiplying both sides of (5.20) by $x^{-\alpha}$ and integrating over I , we have

$$\begin{aligned} \mathcal{R}' &= 2^{-1} \int_I x^{-2\alpha} (z^2(x, t) - 1) dx \mathcal{R} \\ &\leq 2^{-1} \int_I x^{-2\alpha} (z(x, t) - 1) dx \mathcal{R} \\ &\leq 2^{-1} \int_I x^{-\alpha} (z(x, t) - 1) dx \mathcal{R} \\ &\leq (\mathcal{R} - (1 - \alpha)^{-1}) \mathcal{R}. \end{aligned} \quad (5.29)$$

By the comparison principle (cf. [12, Theorem I.4.1]), from (5.29) we conclude that $\mathcal{R}(t) \searrow 0$, as $t \rightarrow \infty$.

The case $\mathcal{R}[z(0, \cdot)] < 0$ is analyzed similarly. \square

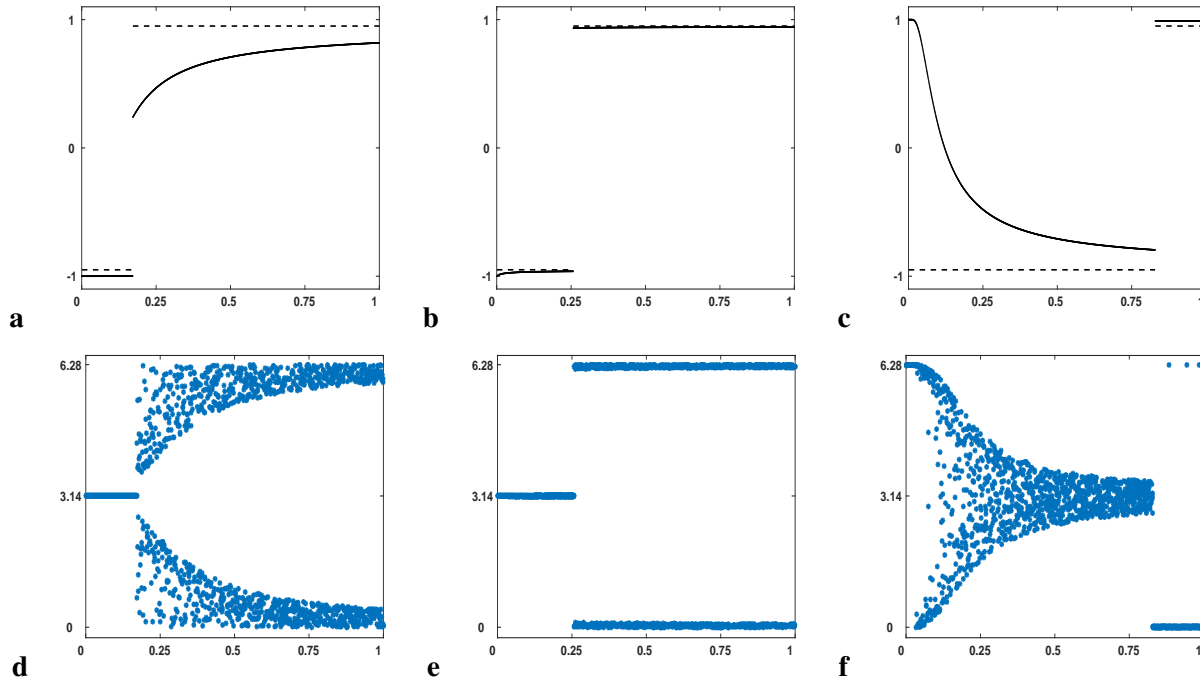


Figure 3: The initial conditions (dashed line) and asymptotic states (solid line) for (5.20) **(a-c)** and the corresponding steady states of (5.2) **(d-f)**. The patterns shown in **(d)** and **(f)** are the examples of chimera states. In **(d)** the oscillators in the left region I^- are localized around π and are spread-out around 0 in the right region I^+ . Similarly, the pattern shown in **(f)** features localized distribution around 0 and the spread-out one around π .

5.5 Attractors of the repulsively coupled model

Theorem 5.4 shows that solutions of the mean field equation of the form (5.19) approach an equilibrium from the set $\{\mathcal{R} = 0\}$. To illustrate possible patterns generated in this scenario, we consider the IVP for (5.20) with the following initial conditions:

$$z_{\delta, x_0}^{(step)}(x) = \begin{cases} -1 + \delta, & x \in I^- := (0, x_0), \\ 1 - \delta, & x \in I^+ := [x_0, 1), \end{cases} \quad (5.30)$$

For $0 < \delta \ll 1$, $z_{\delta, x_0}^{(step)}$ is close to the equilibrium $z_{0, x_0}^{(step)} \in \tilde{\mathcal{E}}_1$, corresponding to a phase locked solution, localized around π for $x \in I^-$ and around 0 for $x \in I^+$.

Consider the IVP for (5.20) with initial condition $z_{\delta, x_0}^{(step)}$ for $0 < \delta < 1$. To this end, note that for $x^* = 2^{\frac{-1}{1-\alpha}} \in (0, 1)$,

$$\int_0^{x^*} y^{-\alpha} dy = - \int_{x^*}^1 y^{-\alpha} dy.$$

Suppose first that $0 < x_0 < x^*$. Then $\mathcal{R}(0) > 0$. By Theorem 5.4, $\mathcal{R}(t) \searrow 0$. Furthermore, $|z(t, x)| \leq 1$ and, thus, $z(t, x)$ is monotonically decreasing in time for every $x \in (0, 1]$. In particular,

$$-1 \leq z(t, x) \leq -1 + \delta, \quad x \in I^- = (0, x_0), \quad t \geq 0. \quad (5.31)$$

This means that in I^- the oscillators remain localized around π (in the moving frame of coordinates) (cf. (5.24)), provided $0 < \delta \ll 1$ (Fig. 3d). On the other hand, in I^+ , $z(t, \cdot)$ is monotonically decreasing to its asymptotic state z_∞ at which $\mathcal{R}(z_\infty) = 0$ (see Fig. 3a). In I^+ , there must be an interval over which z is positive and strictly less than $1 - \delta$ for all times. Denote such interval $\tilde{I}^+ \subset I^+$. Thus, over \tilde{I}^+ , $z(t, x)$ is bounded away from ± 1 by a distance greater than δ uniformly in time. Thus, the oscillators over \tilde{I}^+ exhibit a greater degree of incoherence. The asymptotic state z_∞ contains both the region of coherent dynamics (I^-) and that of incoherent (I^+) (Fig. 3a). Thus, z_∞ corresponds to a chimera state. This is clearly seen in numerics (see Fig. 3d). In the next section, for the modified model we will present tight estimates characterizing the asymptotic state z_∞ .

Next, we comment on the transformation of the asymptotic state z_∞ as x_0 is increasing past x^* . The case of $x > x^*$ presents a symmetric scenario. In this case, $\mathcal{R}(0) < 0$ and both $\mathcal{R}(t)$ and $z(t, \cdot)$ are monotonically increasing (see Fig. 3c). In particular, $1 - \delta \leq z(t, x) \leq 1$ in I^+ for $t \geq 0$, and the oscillators are localized around 0 in I^+ , while exhibiting incoherent behavior in I^- (see Fig. 3c,f). When x_0 is close to x^* , $\mathcal{R}(0)$ is close to zero, and $|\mathcal{R}(t)|$ remains small for all times. This means that the initial pattern does not change much in the process of evolution, and z_∞ remains close to the step function

$$z_{0,x_0}^{(step)}(x) := \pm 1, \quad x \in I^\pm.$$

The equilibrium $z_{0,x_0}^{(step)} \in \tilde{\mathcal{E}}_1$ is unstable but lies close a stable equilibrium $z_{step,x^*} \in \tilde{\mathcal{E}}_2$ (see Fig. 3b,e).

5.6 Chimera states in the modified KM

We now turn to a modification of the KM on power law graphs, for which we derive tight estimates for the chimera states. If instead of scaling the coupling term by $n\rho_n$, as in (2.6), we scale it by the expected degree of node i :

$$d_{ni} = \mathbb{E}_\omega \deg_{\Gamma_n}(i) = \sum_{j=1}^n \bar{W}_{nij},$$

the repulsively coupled KM and the corresponding averaged equation take the following form:

$$\dot{u}_{ni} = \frac{1}{d_{ni}} \sum_{j=1}^n \xi_{nij}(\omega) \sin(u_{ni} - u_{nj}), \quad i \in [n], \quad (5.32)$$

and

$$\dot{v}_{ni} = \frac{1}{n} \sum_{j=1}^n x_{nj}^{-\alpha} \sin(v_{ni} - v_{nj}), \quad i \in [n], \quad (5.33)$$

respectively. The mean field equation then becomes (cf. [15, Example 2.5])

$$\frac{\partial}{\partial t} \rho(t, u, x) + \frac{\partial}{\partial u} \left\{ \rho(t, u, x) \int_I \int_S (1 - \alpha) y^{-\alpha} \sin(u - v) \rho(t, v, y) dv dy \right\}. \quad (5.34)$$

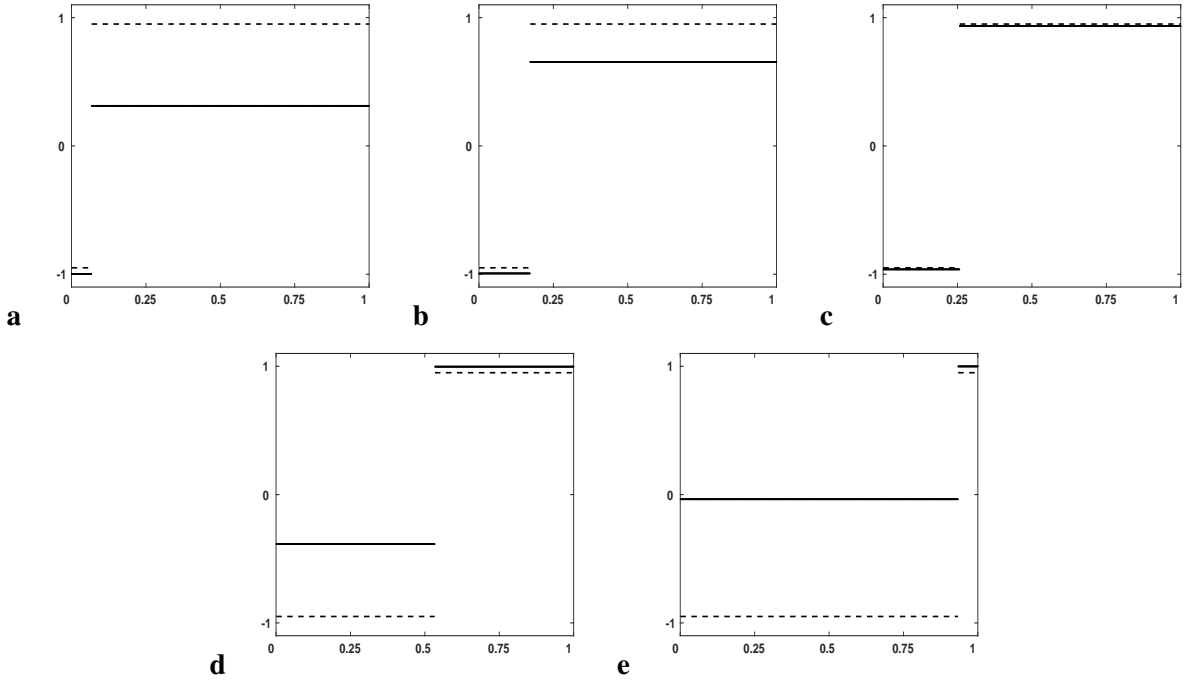


Figure 4: The initial conditions (dashed line) and asymptotic states (solid line) for (5.35).

Applying the Ott-Antonsen Ansatz to the model at hand, we arrive at

$$\dot{z} = \frac{1 - \alpha}{2} (z^2 - 1) \mathcal{R}[z]. \quad (5.35)$$

For (5.35) subject to the initial condition (5.30), below we present tight bounds for the large time asymptotic state z_∞ .

Suppose $\mathcal{R}[z(0, \cdot)] > 0$ and note that (5.35) and (5.30) imply

$$|z(x, t)| \leq 1 \quad \text{and} \quad \mathcal{R}[z(t, \cdot)] \geq 0,$$

for any $x \in I$ and $t \geq 0$. Furthermore, $z(t, x)$ is monotonically decreasing.

On the other hand, from (5.35) we have

$$(1 - \alpha)(z - 1)\mathcal{R}[z(t, \cdot)] \leq \frac{\partial}{\partial t} z \leq \frac{1 - \alpha}{2}(z - 1)\mathcal{R}[z(t, \cdot)]. \quad (5.36)$$

Multiplying all sides of the double inequality (5.36) by $x^{-\alpha}$ and integrating over I , we have

$$((1 - \alpha)\mathcal{R}[z(t, \cdot)] - 1) \leq \frac{\partial}{\partial t} \mathcal{R}[z(t, \cdot)] \leq 2^{-1} ((1 - \alpha)\mathcal{R}[z(t, \cdot)] - 1). \quad (5.37)$$

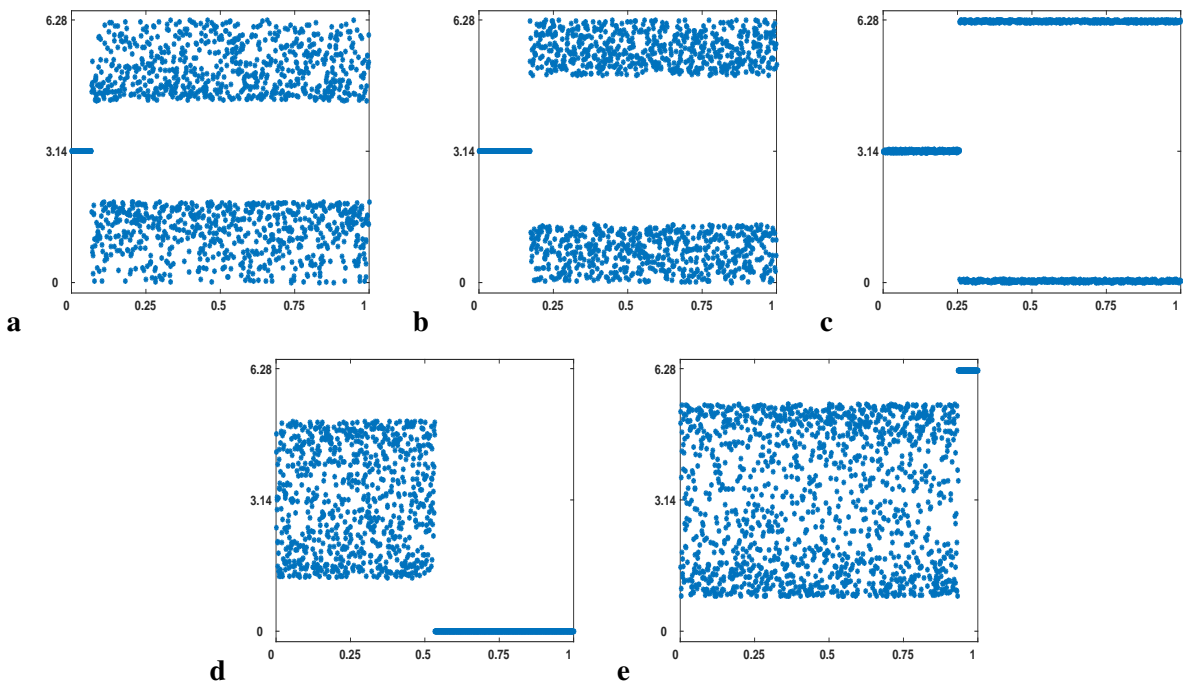


Figure 5: The asymptotic states of (5.32). The patterns in (a-d) correspond to the solutions of (5.35) shown in the corresponding plots of Fig. 4.

Recalling $\mathcal{R}[z(0, \cdot)] > 0$, $\mathcal{R}[z(t, \cdot)] \searrow 0$ as $t \rightarrow \infty$, i.e., $z(t, \cdot)$ approaches an equilibrium from $\tilde{\mathcal{E}}_2$. Next, we characterize the limiting state of the system. Since the initial condition is constant over each of the intervals I^\pm , so is the solution

$$\begin{aligned} z(x, t) &\equiv z^-(t), & x \in I^-, \\ z(x, t) &\equiv z^+(t), & x \in I^+, \end{aligned} \quad (5.38)$$

Since $z^-(0) = -1 + \delta$ and $z^-(t) \geq -1$, we have

$$|z^-(t) + 1| \leq \delta, \quad (5.39)$$

i.e., the solution of the repulsively coupled KM (5.1) remains approximately synchronized over I^- .

Denote

$$z_\infty^\pm := \lim_{t \rightarrow \infty} z^\pm(t).$$

Further, since $\mathcal{R}[z(t, \cdot)] \rightarrow 0$ as $t \rightarrow \infty$, we have

$$z_\infty^+ \int_{x_0}^1 y^{-\alpha} dy = -z_\infty^- \int_0^{x_0} y^{-\alpha} dy.$$

and

$$z_\infty^+ = -z_\infty^- \frac{x_0^{1-\alpha}}{1 - x_0^{1-\alpha}}. \quad (5.40)$$

The combination of (5.39) and (5.40) yields

$$(1 - \delta) \frac{x_0^{1-\alpha}}{1 - x_0^{1-\alpha}} \leq z_\infty^+ \leq \frac{x_0^{1-\alpha}}{1 - x_0^{1-\alpha}}. \quad (5.41)$$

This double inequality combined with (5.39) yields tight estimates for the asymptotic state z_∞ in I^+ . Estimates (5.39) and (5.41) characterize the asymptotic states for initial conditions $\mathcal{R}[z(0, \cdot)] > 0$ (Fig. 4**a,b**). The complementary case $\mathcal{R}[z(0, \cdot)] < 0$ is analyzed similarly.

6 Discussion

The results of this study highlight the effects of the scale free connectivity for the dynamics of large networks. We found that the synchronizability of the KM on sparse power law graphs is at least as good as it is on dense graphs. Moreover, the synchronization threshold can be made arbitrarily low by varying the exponent of the power law degree distribution (cf. (4.3)). The imprint of the power law distribution is clearly seen in the stable chimera-like patterns generated by the repulsively coupled model (Fig. 3 **d,f**). Patterns shown in Fig. 3 and 5 demonstrate a remarkable ability of the attractors of the network to “remember” the initial condition on a continuous scale. Note that by continuously varying the parameter x_0 in the initial condition $z_{\delta, x_0}^{(step)}$ (i.e., by varying the the distribution of the positions of oscillators at time 0), we are effectively changing the asymptotic state z_∞ (Fig. 3 **a-c**) and, therefore, the asymptotic distribution of the oscillators (Fig. 3 **d-f**). The memory of the initial conditions, which for the model at hand can be understood by studying the reduced equation (5.20), appears to be a common feature of nonlocally coupled networks (see also §6.2 in

[21]). In computational neuroscience, there has been a search for mechanisms implementing continuous attractors in network models. The models proposed, as a rule, in this context suffer from the lack of structural stability, i.e., the desired continuous attractor can be destroyed by small perturbations of parameters (see, e.g., [34]). On the other hand, networks of nonlocally coupled oscillators, like the one presented in this paper, provide a robust mechanism for dependence of the attractor on initial conditions on the continuous scale. Finally, the repulsively coupled KM on power law graphs (5.2) and its modification (5.32) provide a new simple mechanism for generating chimera states.

In conclusion, we note that the analysis in Section 5 is done for the averaged equation, which approximates the original model on a random graph on finite time intervals. Therefore, the results for the averaged model reported in this section may hold for the original model only transitively. We believe that these results nonetheless give valuable insights into the dynamics of coupled systems on power law graphs, and the asymptotic states of such systems should be investigated further.

Acknowledgements: This work was supported in part by the NSF DMS 1412066 (GM).

References

- [1] D.M. Abrams and S.H. Strogatz, *Chimera states in a ring of nonlocally coupled oscillators*, Internat. J. Bifur. Chaos Appl. Sci. Engrg. **16** (2006), no. 1, 21–37. MR 2214910 (2006k:37043)
- [2] Albert-László Barabási and Réka Albert, *Emergence of scaling in random networks*, Science **286** (1999), no. 5439, 509–512. MR 2091634
- [3] E. A. Barbašin and N. N. Krasovskii, *On stability of motion in the large*, Doklady Akad. Nauk SSSR (N.S.) **86** (1952), 453–456. MR 0052616
- [4] C. Borgs, J. T. Chayes, H. Cohn, and Y. Zhao, *An L^p theory of sparse graph convergence I: limits, sparse random graph models, and power law distributions*, ArXiv e-prints (2014).
- [5] Christian Borgs, Jennifer Chayes, László Lovász, Vera Sós, and Katalin Vesztegombi, *Limits of randomly grown graph sequences*, European J. Combin. **32** (2011), no. 7, 985–999. MR 2825531
- [6] Hayato Chiba, *A proof of the Kuramoto conjecture for a bifurcation structure of the infinite-dimensional Kuramoto model*, Ergodic Theory Dynam. Systems **35** (2015), no. 3, 762–834. MR 3334903
- [7] Hayato Chiba and Georgi S. Medvedev, *The mean field analysis of the Kuramoto model on graphs I. The mean field equation and the transition point formulas*, submitted.
- [8] Hayato Chiba and Isao Nishikawa, *Center manifold reduction for large populations of globally coupled phase oscillators*, Chaos **21** (2011), no. 4, 043103, 10. MR 2918832
- [9] Fan Chung and Linyuan Lu, *The average distances in random graphs with given expected degrees*, Proc. Natl. Acad. Sci. USA **99** (2002), no. 25, 15879–15882. MR 1944974
- [10] R. M. Dudley, *Real analysis and probability*, Cambridge Studies in Advanced Mathematics, vol. 74, Cambridge University Press, Cambridge, 2002, Revised reprint of the 1989 original. MR 1932358
- [11] François Golse, *On the dynamics of large particle systems in the mean field limit*, Macroscopic and large scale phenomena: coarse graining, mean field limits and ergodicity, Lect. Notes Appl. Math. Mech., vol. 3, Springer, [Cham], 2016, pp. 1–144. MR 3468297
- [12] Philip Hartman, *Ordinary differential equations*, S. M. Hartman, Baltimore, Md., 1973, Corrected reprint. MR 0344555
- [13] Frank C. Hoppensteadt and Eugene M. Izhikevich, *Weakly connected neural networks*, Applied Mathematical Sciences, vol. 126, Springer-Verlag, New York, 1997. MR 1458890
- [14] Roger A. Horn and Charles R. Johnson, *Matrix analysis*, second ed., Cambridge University Press, Cambridge, 2013. MR 2978290
- [15] Dmitry Kaliuzhnyi-Verbovetskyi and Georgi S. Medvedev, *The Semilinear Heat Equation on Sparse Random Graphs*, SIAM J. Math. Anal. **49** (2017), no. 2, 1333–1355. MR 3634990
- [16] N. N. Krasovskii, *Nekotorye zadachi teorii ustoichivosti dvizheniya.*, Gosudarstv. Izdat. Fiz.-Mat. Lit., Moscow, 1959. MR 0106313

- [17] Y. Kuramoto and D. Battogtokh, *Coexistence of coherence and incoherence in nonlocally coupled phase oscillators*, *Nonlinear Phenomena in Complex Systems* **5** (2002), 380–385.
- [18] Yoshiki Kuramoto, *Self-entrainment of a population of coupled non-linear oscillators*, *International Symposium on Mathematical Problems in Theoretical Physics* (Kyoto Univ., Kyoto, 1975), Springer, Berlin, 1975, pp. 420–422. *Lecture Notes in Phys.*, 39. MR 0676492
- [19] C. Lancellotti, *On the Vlasov limit for systems of nonlinearly coupled oscillators without noise*, *Transport Theory Statist. Phys.* **34** (2005), no. 7, 523–535. MR 2265477 (2007f:82098)
- [20] J. LaSalle, *Some extensions of liapunov's second method*, *IRE Transactions on Circuit Theory* **7** (1960), no. 4, 520–527.
- [21] Georgi S. Medvedev, *The nonlinear heat equation on dense graphs and graph limits*, *SIAM J. Math. Anal.* **46** (2014), no. 4, 2743–2766. MR 3238494
- [22] ———, *The nonlinear heat equation on W -random graphs*, *Arch. Ration. Mech. Anal.* **212** (2014), no. 3, 781–803. MR 3187677
- [23] ———, *Small-world networks of Kuramoto oscillators*, *Phys. D* **266** (2014), 13–22. MR 3129708
- [24] Georgi S. Medvedev and Xuezhi Tang, *Stability of twisted states in the Kuramoto model on Cayley and random graphs*, *J. Nonlinear Sci.* **25** (2015), no. 6, 1169–1208. MR 3415044
- [25] Georgi S. Medvedev and J. Douglas Wright, *Stability of Twisted States in the Continuum Kuramoto Model*, *SIAM J. Appl. Dyn. Syst.* **16** (2017), no. 1, 188–203. MR 3600363
- [26] G.S. Medvedev, *Stochastic stability of continuous time consensus protocols*, *SIAM Journal on Control and Optimization* **50** (2012), no. 4, 1859–1885.
- [27] Sebastien Motsch and Eitan Tadmor, *Heterophilious dynamics enhances consensus*, *SIAM Rev.* **56** (2014), no. 4, 577–621. MR 3274797
- [28] H. Neunzert, *Mathematical investigations on particle - in - cell methods*, vol. 9, 1978, pp. 229–254.
- [29] Simbarashe Nkomo, Mark R. Tinsley, and Kenneth Showalter, *Chimera and chimera-like states in populations of nonlocally coupled homogeneous and heterogeneous chemical oscillators*, *Chaos* **26** (2016), no. 9, 094826, 10. MR 3550289
- [30] O.E. Omelchenko, *Coherence-incoherence patterns in a ring of non-locally coupled phase oscillators*, *Nonlinearity* **26** (2013), no. 9, 2469.
- [31] E. Ott and T. M. Antonsen, *Low dimensional behavior of large systems of globally coupled oscillators*, *Chaos* (2008), no. 18, 037113.
- [32] Mark J. Panaggio and Daniel M. Abrams, *Chimera states: coexistence of coherence and incoherence in networks of coupled oscillators*, *Nonlinearity* **28** (2015), no. 3, R67–R87. MR 3319380
- [33] Mason A. Porter and James P. Gleeson, *Dynamical systems on networks*, *Frontiers in Applied Dynamical Systems: Reviews and Tutorials*, vol. 4, Springer, Cham, 2016, A tutorial. MR 3468887

- [34] H. Sebastian Seung, *Continuous attractors and oculomotor control*, Neural Networks **11** (1998), no. 78, 1253 – 1258.
- [35] Steven H. Strogatz, *From Kuramoto to Crawford: exploring the onset of synchronization in populations of coupled oscillators*, Phys. D **143** (2000), no. 1-4, 1–20, Bifurcations, patterns and symmetry. MR 1783382
- [36] Daniel A. Wiley, Steven H. Strogatz, and Michelle Girvan, *The size of the sync basin*, Chaos **16** (2006), no. 1, 015103, 8. MR 2220552